

# Theory of High Performance Piezotronic Quantum Harmonic Oscillator under Nonuniform Strain

Yaming Zhang<sup>1</sup>, Jiaheng Nie<sup>1</sup>, Ruhao Liu<sup>1</sup>, Baohua Teng<sup>1,\*</sup>, Lijie Li<sup>2,\*</sup> and Yan

Zhang<sup>1,3,4,\*</sup>

<sup>1</sup> *School of Physics, University of Electronic Science and Technology of China, Chengdu 610054, China*

<sup>2</sup> *Multidisciplinary Nanotechnology Centre, College of Engineering, Swansea University, Swansea, SA1 8EN, UK*

<sup>3</sup> *Beijing Institute of Nanoenergy and Nanosystems, Chinese Academy of Sciences, Beijing 100083, China*

<sup>4</sup> *College of Nanoscience and Technology, University of Chinese Academy of Sciences, Beijing 100049, China*

\* To whom correspondence should be addressed, E-mail: [phytbh@163.com](mailto:phytbh@163.com), [L.Li@swansea.ac.uk](mailto:L.Li@swansea.ac.uk) and [zhangyan@uestc.edu.cn](mailto:zhangyan@uestc.edu.cn)

## Abstract

Piezotronics and piezo-phototronics are two emerging fields that involve high performance piezoelectric semiconductor devices. The nonuniform strain can create nonlinear piezopotential even in nonpiezoelectric materials such as silicon. Here, we propose theory of quantum piezotronics under nonuniform strain using a typical example of the interaction between independently trapped charges under nonlinear piezopotential. The trapped-ion motional frequency along the x direction can increase from 4 MHz to 25 MHz, and the electricfield noise can decrease by 15 times under nonuniform strain. This piezotronic harmonic oscillator based on trapping wells not only provides a good understanding of quantum piezotronics but also a guide for developing peizotronic devices for quantum computing.

**Keywords:** piezotronics; nonuniform strain; trapped ion; harmonic oscillators; qubit

## 1. Introduction

Piezotronics and piezo-photronics are two emerging fields for couplings of piezoelectric, semiconductor and photoexcitation[1, 2]. High-performance piezotronic and piezo-phototronic devices are fabricated using piezoelectric semiconductors, such as nanogenerators[3-5], strain sensor[6], solar cell[7], light-emitting diodes[8], and photodetectors[9]. The mechanism of piezotronic transistors is that polarization induced by strain significantly modulates built-in field in the p-n junction or the Schottky barrier in metal semiconductor contact[10]. Ultrahigh sensitivity piezo-phototronic devices have been fabricated based on single-layer MoS<sub>2</sub> and ZnO nanowires[11-13]. The piezoelectric field can be used to change quantum states of topological insulator[14]. Recently, the nonuniform strain can be used to improve piezoelectric polarization [15], even in nonpiezoelectric semiconductor[15, 16].

The trapped-ion system is a good qubit candidate for quantum simulation and quantum information processing (QIP) [17-21]. In recent years, the experimental breakthroughs have been made by using trapped ions formed by a good approximation harmonic based on a combination of the static and radio-frequency (RF) quadrupole potentials[22, 23]. In such devices, the effective harmonic potential is given by pseudopotential approximation, in which a single trapped ion can be as a simple harmonic oscillator[24-27]. Therefore, the qubits can be formed in trapped ions based on other setup, where the potential near trap center is assumed as purely quadratic[28, 29]. Strain-induced polarization can be used to form trapped ions on piezoelectric semiconductors[1, 2]. Piezoelectric semiconductor with surtzite structure are good candidates such as GaN[30, 31]. Since trapped ions in trapped wells can be coupled not only by Coulomb interaction, but also nonlinear piezopotential (via energy exchange), the proposed system is ideal for QIP, and thus for small quantum computers[32-35]. By turning motion of two trapped ions into resonance, the ion energy is exchanged between the trapped ions at the quantum levels, establishing a directly coupling for the trapped ions[28]. Recently, the fabrication of trapped-ion system and trappedion QIP have been achieved[23, 33, 35-42]. The two basic problems need to be solved before trapped ions is used for QIP and to operate trapped ions as proposed in refs [21, 43]. (1) It is difficult to generate a purely quadratic potential in trapped wells due to the machined difficulty of perfectly hyperbolic electrodes. The situation of trapping potential makes it hard to remain harmonic[21, 22]. (2) Owing to the surface electric field noise (SEFN)[21, 44-46] that exists in trapped-ion system, this is non-trivial to generate two-qubit gates using energy exchange coupling for oscillation in coupled trapping wells. The attempt can be made to solve problem (1), the effective harmonic potential is as quadratic[47], a quadratic potential can be created by PS based on nonuniform strain[30, 48]. High motional frequencies can be made to solve problem (2), many experiments show that the electric-field noise spectrum varies with the power law, i.e.  $S_E(\omega) \propto \omega^\alpha$  with a range between -1.5 and -1.0[21, 43, 49-51].

We propose a solution that can solve the problems (1) and (2) at once. Similar to ref. [43, 52], we choose to control motion of trapped ions by using piezoelectric potential in wurtzite GaN thin film, as shown in Fig. 1. We assume two trapping wells to exist along trap x axis. It is by now feasible to experimentally control motional frequency of trapping ions on resonance condition[22, 53]. These are preferably of ion or of electron type. The trapped ions are oscillating, that is the necessary condition for the appearance of energy exchange coupling for quantized mechanical oscillators in trapping wells, and thus for the use of trapped ions for qubits[22, 23]. Nonlinear piezo-potential in GaN can be coupled between two independently trapped ions. This strong coupling mechanism is that the nonlinear piezo-potential affects ions oscillating processes and directly effect on the coupling strength between trapped ions. Single-ion motional frequency along the x direction can change from 4 MHz to 25 MHz under nonuniform strain. The electric-field noise is decreased by 6-15 times under nonuniform strain.

## 2. Model of Quantum Piezotronic Trapped Ions under Nonuniform Strain

Take a typical two independently trapped ions for qubit as example, a wurtzite GaN thin film that is assumed as rectangular with length L and width W, as shown in Fig. 1. In piezoelectric semiconductor, a nonuniform strain can create a nonlinear piezo-potential which tune trapped wells in the x direction. The oscillator of two trapped ions (with charges  $q_a$  and  $q_b$ , and energy E, with respect to the oscillating state) separated by a distance  $s_0$  in such a set-up are described by Schrodinger equations[22, 54]

$$\left( \frac{p_i^2}{2m_{0,i}} + U \right) \psi = E\psi \quad (1)$$

$$U(x_a, x_b) = \frac{1}{4\pi\epsilon_0} \frac{q_a q_b}{s_0 - x_a + x_b} \approx \frac{1}{4\pi\epsilon_0} \frac{q_a q_b}{s_0} \left( 1 + \frac{x_a - x_b}{s_0} + \frac{x_a^2}{s_0^2} + \frac{x_b^2}{s_0^2} - \frac{2x_a x_b}{s_0^2} \right)$$

where the trapping potential is assumed to vary stepwise,  $U = U(x_a, x_b)$  in trapping wells. In equation (1),  $x_a$  and  $x_b$  are the displacement of the ions from external potential minima.  $m_{0,i}$  is the ion mass,  $p_i$  is momentum operator, and  $\epsilon_0$  is vacuum permittivity. The second term represents a steady force between the ions that displaces them slightly; if necessary, it can be counteracted with additional potentials applied to nearby electrodes. The terms proportional to  $x_a^2$  and  $x_b^2$  represent static change in the trap frequencies, it can be compensated by potentials applied to nearby electrodes. The term proportional to  $x_a x_b$  represents the lowest-order coupling between the ion's motions. The appropriate harmonic oscillating conditions for such a wave function have been formulated in ref. and can be written as[54]

$$\psi_n(x) = \left( \frac{m_{0,i}\omega_{0,i}}{\pi\hbar} \right)^{1/4} \frac{1}{\sqrt{2^n n!}} H_n \left( \sqrt{\frac{m_{0,i}\omega_{0,i}}{\pi\hbar}} x \right) e^{-\frac{m_{0,i}\omega_{0,i}x^2}{2\hbar}} \quad (2)$$

corresponding to the axis  $x$  of the ion-wire-ion system shown in Fig. 1, where  $H_n$  is Hermite polynomials. The  $\omega_{0,i}$  in equation (2) (and in equation (3) below) is motional frequency of trapped ions. The  $i$  signs in equation (2) (and in equation (3) below) is the choices of trapped ion. The full set of steady-state solutions of equation (1) can be readily determined[54]. The boundary condition yields the following quantized energy  $E_n$  for quantized mechanical oscillators in the  $x$  direction[23, 54]

$$E_n = \left(n + \frac{1}{2}\right)\hbar\omega_{0,i} \quad (3)$$

The level spacing of the equation (3) is estimated as  $\Delta E = \hbar\omega_{0,i}$ , which give  $\Delta E \approx 4.6$  neV, where we used  $\omega_i/2\pi \approx 4.04$  MHz and assumed two trapped-ions motion into resonance condition. The equation (3) can determine energy gap for excitations as  $E_{gap} = \hbar\omega_{0,i}$ . Therefore, this gap is 4.6 neV, which is small for trapped ions. It is a unique feature of trapped ions that can allow for coupling between two independently trapped ions as will be discussed below.

The ground solutions are calculated at  $n=0$  in equation (3) under nonuniform strain. By utilizing a mathematical derivation in Appendix A, the corresponding nonlinear piezo-potential  $V_{piezo}$  can be expressed relative to the strain gradient  $s_{33,3}$  as

$$V_{piezo} = \frac{e_{33}s_{33,3}}{2\epsilon_s\epsilon_0} x^2 \quad (4)$$

Here, the  $e_{33}$  and  $\epsilon_s$  is piezoelectric constant and relative dielectric constant. For oscillating state to be tuned at nonuniform strain, we require that  $V_{piezo} > 0$ , which implied that the motional frequency ( $\omega_{0i,piezo}$ ) of trapped ions in the  $x$  direction, given by

$$\omega_{0i,piezo} = \sqrt{\omega_{0i}^2 + \frac{qe_{33}s_{33,3}}{\epsilon_s\epsilon_0 m_{0i}}} \quad (5)$$

is increased. In the trapped wells, the motional frequency of trapped ions  $\omega_{0i}$  along the  $x$  direction is influenced by  $V_{piezo}$ . Again the  $i$  sign refers to trapped ion A and B. In the following, we will focus on coupling rate scale  $\Omega_{ex}$  to two trapped ions.

As the equation (1) shows the coupling of ions' motion, the matching condition at small deviations from equilibrium allows us to obtain the equation for  $\Omega_{ex}$  [22, 28]

$$\Omega_{ex} \equiv \frac{q_a q_b}{4\pi\epsilon_0 s_0^3 \sqrt{m_a m_b} \sqrt{\omega_{0a} \omega_{0b}}} \quad (6)$$

with  $\Omega_{ex} \propto 1/s_0^3$ . Equation (6) determines the coupling rate scales for trapped ions. At time  $t = \tau_{ex} = \pi/2\Omega_{ex}$ , the operators have changed a phase factor, and the oscillators have completely exchanged energies, regardless of the initial states. At  $t = 2\tau_{ex}$ , the energies are returned to the initial values in each ion. We now analyse the coupling rate for trapped ions (the resonance condition) under nonuniform strain. In the corresponding nonlinear piezo-potential  $V_{piezo} = \frac{e_{33}s_{33,3}}{2\varepsilon_s\varepsilon_0}x^2$ , we can rewrite equation (6) considerably, obtaining

$$\begin{aligned}\frac{\Omega_{ex,piezo}}{\Omega_{ex}} &\equiv \frac{\omega_0}{\sqrt{\omega_0^2 + \frac{qe_{33}s_{33,3}}{\varepsilon_s\varepsilon_0 m_0}}} \quad s_{33,3} > 0 \\ &= 1 - 2\pi e_{ijk} k_{jkl} s_0^3 / \varepsilon_s q \quad s_{33,3} \geq 0\end{aligned}\tag{7}$$

The trapped ion can be treated as a single harmonic oscillator, the potential nearby trap center can be assumed as purely quadratic[21]. The nonuniform strain can generate quadratic piezo-potential in piezoelectric materials[30, 55, 56]. The quadratic potential generated by nonuniform strain is used to control the trapped ions motional frequency. The piezo-potential is approximately linear along polar direction under uniform strain[57-59].

The piezoelectric semiconductor films can generate piezo-potential to replace dc electrodes under nonuniform strain. The separation of the trapped ions and curvatures of the trapping wells can be varied by applying static potential to the direct current electrodes[22]. Confinement along the trap axis is achieved by applying direct current voltages ranging from 15 V to 15 V to the direct current electrodes[60, 61]. The piezo-potential of GaN can arrive 6 V under a -0.12% compressive strain, the potential difference is approximately 10 V[57]. Therefore, the dc voltage can be replaced under nonuniform strain due to potential far larger than uniform strain case.

The principle of such traps is by using combination of static and RF quadrupole potentials to confine the charged particles in three spatial directions[21]. The trap RF potential over 100 V at  $\sim 10\text{--}100\text{ MHz}$ , are applied to the RF electrode[18, 21, 43, 60, 61]. Piezoelectric materials under the high-frequency dynamic strain can be used to replace radio-frequency (RF) source. ZnO thin film can be used to design surface acoustic wave (SAW)[62]. The GaN-based multi-mode composite high-overtone bulk acoustic wave resonator (HBAR) is as a widely used phonon source. For instance, the electrically actuated GaN/NbN/SiC epi-HBAR can be integrated with SiC-based spin qubits[63], and measurements on the epitaxially grown HBARs show high Q values up to 13.6 million at a frequency of 10 GHz at 7.2 K. The output voltage of BaTiO<sub>3</sub>P(VDF-HFP) composite film can arrive over 110 V under a compressive force of  $\sim 0.23\text{ MPa}$  perpendicular to the surface in previous work[64]. The output voltage of PZT thin film and nanowire array can arrive 165 V[65] and 209 V[66], respectively. Phonon vibration frequency can reach over GHz for PZT[67, 68] and BaTiO<sub>3</sub> [69, 70].

### 3. Results and Discussion

Figure 2(a) shows energy bands and wave function of quantized harmonic oscillator as well as the change of energy bands and wave function with positive/negative strain gradient. The energy bands are rise under positive strain gradient, is drop under negative strain gradient. The wave function is narrow under positive strain gradient, is expanded under negative strain gradient. The quantized harmonic oscillator case shows the nonlinear piezo-potential to couple quantized mechanical oscillator. A series of solutions to quantized harmonic oscillator for motional frequency ( $\omega_0 = 4.04$  MHz) are shown in Fig. 2(b). The level spacing of quantized harmonic oscillator increases as  $\omega_0$  increases, and have a linear parameter dependence. It is estimated as  $\Delta E = \hbar\omega_{0,i}$ , that is in range of a few tens of n eV as mentioned in equation (3). Figure 2(c) shows an example of a wavefunction. that is the ground-state solution for parameter choice of motional frequency  $\omega_0/2\pi=4.04$  MHz, strain gradient choice  $s_{33,3} = 0$  or  $s_{33,3} = 0.2$ . The distribution of the wavefunction on the  $s_{33,3} = 0$  and  $s_{33,3} = 0.2$  is different. Ground-state solutions (the red lines in Fig.2(b)) have change under strain gradient-similar to the problem of quantized mechanical oscillators that obey the time-independent Schrodinger equation. Figure 2 (a) shows the excited-state solutions do have influence under strain gradient.

The oscillating state in the two trapped ions can be coupled via Coulomb interaction, as shown in Fig. 1. Because in the fixed value of  $s_0$ , the coupling  $\Omega_{ex}$  depends only strongly on motional frequency of trapped ions. For bound-state solutions with  $s_{33,3} > 0$ , a coupling over a frequency exceeding some times the initial motional frequency is possible. For the case where two ground states couple in trapped ions, the coupling rate is lower for trapped ions ( $\omega_0/2\pi=4.04$  MHz,  $s_{33,3} = 0.2$ ), as shown in Fig. 2(d). If we couple nonlinear piezopotential with motion of two independently trapped ions, the motional frequency  $\omega_{0,i}$  can be even larger.

For the case of coupling two quantized harmonic oscillators separated by Coulomb interaction, each oscillator is a trapped Be+ ion, as shown in Fig. 1. It is interesting that the two oscillators can completely swap their energy, regardless of the original states at  $t = \tau_{ex} = \pi/2\Omega_{ex}$ . The energies can return to the original states of each ion at  $t = 2\tau_{ex}$ . The coupling rate scales is as  $\Omega_{ex} \propto 1/\sqrt{\omega_a}$  or  $1/\sqrt{\omega_b}$ . The axis motional frequency of ion can be controlled by strain gradient, also allowing a tunable interaction of  $\Omega_{ex}/\pi$  and  $\tau_{ex}$ . Figure 3(a) shows the strain is approximately linear distribution along transverse direction under point force. Figure 3(b) shows time of swapped ion's energy ( $\tau_{ex}$ ) is increased from 162  $\mu$ s to 977  $\mu$ s for  $\omega_0/2\pi=4.04$  MHz under strain gradient. The  $\tau_{ex}$  can be increased with increase of motional frequency. Under strain gradient, the coupling rate ( $\Omega_{ex}$ ) is decreased from 3.1 KHz to 0.51 KHz. The  $\Omega_{ex}$  can be decreased with increasing motional frequency, indicated by Fig.3(c). Figure 3(d) shows the SEFN is decreased by 6-15 times under strain gradient. The quadratic piezo-potential can control the motional frequency of trapped ions. The electric-field noise spectrum varies with the power law, i.e.  $S_E \propto \omega^\alpha$  with a range between -1.5 and -1. The piezo-potential can decrease SEFN by increasing ion's motional frequency. The quantum piezotronics based on nonuniform strain can decrease influence of SEFN on the coherence of the ion motion.

Figure 4 shows influence of the separated distance of ions ( $s_0$ ) on the physical characteristic of trapped ions. Figure 4(a) shows the motional frequency is increased with decrease of  $s_0$ . The mass of ion can influence motional frequency of ions, large mass can decrease motional frequency. Figure 4(b) shows  $\tau_{ex}$  is increased by increasing  $s_0$ . Similar to Fig. 3(b), the high motional frequency can increase  $\tau_{ex}$ . Figure 4(c) shows  $\Omega_{ex}$  is decreased by increasing  $s_0$ . Similar to Fig. 3(c), the high motional frequency can decrease  $\Omega_{ex}$ . Figure 4(d) shows the SEFN is decreased with increase of  $s_0$ . The ion's mass can influence SEFN, the large ion's mass increases SEFN.

The surfaces of the metal electrodes and the nearby insulators play a core role in ion heating via SEFN[43]. The experiments find the SEFN spectrum varies as a power law with respect motional frequency  $\omega$ , i.e.  $S_E \propto \omega^\alpha$  [21]. Recent, the measurements found  $\alpha$  in much narrower range, i.e between -1.5 and -1[43, 49-51]. The nonuniform strain can generate nonlinear piezo-potential in piezoelectric materials[30], in which the piezo-potential can be coupled between the trapped ions. Ion motional frequency is theoretically increased from 4 MHz to 25 MHz. The SEFN is decreased by 15 times.

The point force can induce local nonuniform strain by using an atomic force microscope tip[15, 16, 71]. The diamond anvil cell can be used to generate high pressure[72-74]. The strain gradient can be generated from the disclinations (BiFeO<sub>3</sub> nanostructures array on LaAlO<sub>3</sub> substrates through a high deposition flux)[30]. The strain distribution can be identified by geometric phase analysis (GPA) or grazing incident X-ray diffraction (GIXRD) measurements. Using quantitative high-resolution electron microscopy, the strain fields (in-plane, shear, and out-of-plane) of edge-type misfit dislocations can be visualized by using GPA[75, 76]. The in-plane strain gradient distribution perpendicular to the substrate is identified by GIXRD - measurements[77].

This principle can be used to apply nonuniform strain on other piezotronics and piezophototronic devices. The non-piezoelectric semiconductor (Si, TiO<sub>2</sub>, and Nb-SrTiO<sub>3</sub>) is used for piezotronic transistor by using nonuniform strain[15, 16]. Nonuniform strain can be used for designing ultrahigh performance piezotronic devices by enhance piezotronic effect[78]. Nonuniform piezo-phototronic effect is caused by the gradient stress in the micro-disk LED, this results in a wavelength shift of 16 meV for the light emitted[79].. The strain gradient leads to the large built-in electric field of MV/m, and gives rise to huge enhancement of solar absorption[30]. The perovskite solar cell can reach the power conversion efficiency of 20.7% by modulating the strain gradient through strain engineering[77].

#### 4. Summary

Two trapped ions model as quantized harmonic oscillator coupling by the Coulomb interaction is studied. The bound-state of quantum particle are influenced by nonlinear piezopotential. Nonlinear piezo-potential can be solved based on Poisson equation for piezoelectric semiconductors under nonuniform strain. The remarkable new feature of the proposed quantum piezotronics based on nonuniform strain is that, it is possible to couple nonlinear piezo-potential and harmonic oscillators. The allowed energy of quantized harmonic

oscillators can increase 40 times under nonuniform strain. The surface electric-field noise is decreased by 6-15 times under nonuniform strain. This interesting feature can be used for applications of quantum piezotronics under nonuniform strain.

### **Acknowledgments**

The authors are thankful for the support from Major Project of National Natural Science Foundation of China (Grant No. 52192612, 52192610). The authors are thankful for the support from University of Electronic Science and Technology of China (Grant No. ZYGX2021YGCX001).

## Appendix A

The polarization vector of piezoelectric semiconductor film is described by basic equation of piezoelectric theories<sup>[10]</sup>

$$P = e_{ijk} s_{jk}(l) \quad (\text{A1})$$

where  $P$  is the piezoelectric charges,  $e_{ijk}$  and  $s_{jk}(l)$  is piezoelectric constant and nonuniform strain. The Poisson equation can be used to describe the electrostatic behavior of piezoelectric charges.

$$\nabla^2 V_{\text{piezo}} = -q \frac{\rho_{\text{piezo}}(l)}{\epsilon_s} \quad (\text{A2})$$

The  $V_{\text{piezo}}$  and  $\epsilon_s$  is piezo-potential and dielectric constant, the  $\rho_{\text{piezo}}$  is the density distribution of piezoelectric charges. Under nonuniform strain, the  $\rho_{\text{piezo}}$  is given by<sup>[80]</sup>

$$q \rho_{\text{piezo}} = -\nabla \cdot P = -e_{ijk} s_{jk,l} \quad s_{jk,l} = \frac{\partial s_{jk}}{\partial l} \quad (\text{A3})$$

where  $s_{jk,l}$  is the strain gradient tensor, which is defined as gradient of machinal strain  $s_{jk}$ . Substituting equation (3) to (2), the piezo-potential yields the following conditions in the  $l$  direction.

$$V_{\text{piezo}}(l) = \frac{e_{ijk} s_{jk,l}}{2\epsilon_s} \cdot l^2 \quad (\text{A4})$$

Equation (4) determines the piezo-potential distribution under nonuniform strain for piezoelectric semiconductors. The piezo-potential shows nonlinear distribution for the piezoelectric semiconductors in the  $l$  direction. It is apparent that nonuniform strain yields enhancement for piezotronic effect.

## Reference

- [1] W. Wu and Z.L. Wang, Nature Reviews Materials. 1, (2016). <http://doi.org/10.1038/natrevmats.2016.31>
- [2] Z.L. Wang, W. Wu and C. Falconi, MRS Bulletin. 43, 922 (2018). <http://doi.org/10.1557/mrs.2018.263>
- [3] Z.L. Wang and J. Song, Science. 312, 242 (2006). <http://doi.org/10.1126/science.1124005>
- [4] X. Wang, J. Song, J. Liu, and Z.L. Wang, Science. 316, 102 (2007). <http://doi.org/10.1126/science.1139366>
- [5] Y. Qin, X. Wang and Z.L. Wang Nature. 451, 809 (2008). <http://doi.org/10.1038/nature06601> [6] J. Zhou., Y. Gu., P. Fei., W. Mai., Y. Gao., R. Yang., G. Bao., and Z.L. Wang., Nano letters. 8, 3035 (2008).
- [7] Y. Hu, Y. Zhang, Y. Chang, Robert L. Snyder, and W. Zhong Lin, ACS Nano. 4220 (2010).
- [8] Q. Yang, W. Wang, S. Xu, and Z.L. Wang, Nano Lett. 11, 4012 (2011). <http://doi.org/10.1021/nl202619d>
- [9] Q. Yang, X. Guo, W. Wang, Z. Yan, X. Sheng, L. Der Hsien, and W. Zhong Lin, Acs Nano. 4, 6285 (2010).
- [10] Y. Zhang, Y. Liu and Z.L. Wang, Adv Mater. 23, 3004 (2011). <http://doi.org/10.1002/adma.201100906>
- [11] Y. Zhang and L. Li, Nano Energy. 22, 533 (2016). <http://doi.org/10.1016/j.nanoen.2016.02.039>
- [12] L. Li and Y. Zhang, Nano Research. 10, 2527 (2017). <http://doi.org/10.1007/s12274-017-1457-y>
- [13] Y. Zhang, J. Nie and L. Li, Nano Research. 11, 1977 (2018). <http://doi.org/10.1007/s12274-017-1814x>
- [14] G. Hu, Y. Zhang, L. Li, and Z.L. Wang, ACS Nano. 12, 779 (2018). <http://doi.org/10.1021/acsnano.7b07996>
- [15] L. Wang, S. Liu, X. Feng, C. Zhang, L. Zhu, J. Zhai, Y. Qin, and Z.L. Wang, Nat Nanotechnol. 15, 661 (2020). <http://doi.org/10.1038/s41565-020-0700-y>
- [16] D. Guo, P. Guo, L. Ren, Y. Yao, W. Wang, M. Jia, Y. Wang, L. Wang, Z.L. Wang, and J. Zhai, Science Advances. 9, eadd3310 (2023).
- [17] J.A. Devlin, M.J. Borchert, S. Erlewein, M. Fleck, J.A. Harrington, B. Latacz, J. Warncke, E. Wursten, M.A. Bohman, A.H. Mooser, C. Smorra, M. Wiesinger, C. Will, K. Blaum, Y. Matsuda, C. Ospelkaus, W. Quint, J. Walz, Y. Yamazaki, and S. Ulmer, Physical Review Letters. 126, (2021). <http://doi.org/10.1103/PhysRevLett.126.041301>
- [18] J.P. Gaebler, T.R. Tan, Y. Lin, Y. Wan, R. Bowler, A.C. Keith, S. Glancy, K. Coakley, E. Knill, D. Leibfried, and D.J. Wineland, Phys Rev Lett. 117, 060505 (2016). <http://doi.org/10.1103/PhysRevLett.117.060505>

- [19] C.J. Ballance, T.P. Harty, N.M. Linke, M.A. Sepiol, and D.M. Lucas, Phys Rev Lett. 117, 060504 (2016). <http://doi.org/10.1103/PhysRevLett.117.060504>
- [20] R. Srinivas, S.C. Burd, H.M. Knaack, R.T. Sutherland, A. Kwiatkowski, S. Glancy, E. Knill, D.J. Wineland, D. Leibfried, A.C. Wilson, D.T.C. Allcock, and D.H. Slichter, Nature. 597, 209 (2021). <http://doi.org/10.1038/s41586-021-03809-4>
- [21] M. Brownnutt, M. Kumph, P. Rabl, and R. Blatt, Reviews of Modern Physics. 87, 1419 (2015). <http://doi.org/10.1103/RevModPhys.87.1419>
- [22] K.R. Brown, C. Ospelkaus, Y. Colombe, A.C. Wilson, D. Leibfried, and D.J. Wineland, Nature. 471, 196 (2011). <http://doi.org/10.1038/nature09721>
- [23] D. An, A.M. Alonso, C. Matthiesen, and H. Haffner, Phys Rev Lett. 128, 063201 (2022). <http://doi.org/10.1103/PhysRevLett.128.063201>
- [24] D.J. Wineland, C. Monroe, W.M. Itano, D. Leibfried, B.E. King, and D.M. Meekhof, Journal of research of the National Institute of Standards and Technology. 103, 259 (1998).
- [25] J.I. Cirac and P. Zoller, Nature. 404, 579 (2000).
- [26] J.N. Tan. *Interacting ion oscillators in contiguous confinement wells.* in *APS Division of Atomic, Molecular and Optical Physics Meeting Abstracts.* 2002.
- [27] G. Ciaramicoli, I. Marzoli and P. Tombesi, Phys Rev Lett. 91, 017901 (2003). <http://doi.org/10.1103/PhysRevLett.91.017901>
- [28] M. Harlander, R. Lechner, M. Brownnutt, R. Blatt, and W. Hansel, Nature. 471, 200 (2011). <http://doi.org/10.1038/nature09800>
- [29] N. Daniilidis, T. Lee, R. Clark, S. Narayanan, and H. Häffner, Journal of Physics B: Atomic, Molecular and Optical Physics. 42, (2009). <http://doi.org/10.1088/0953-4075/42/15/154012>
- [30] Y.L. Tang, Y.L. Zhu, Y. Liu, Y.J. Wang, and X.L. Ma, Nature Communications. 8, (2017). <http://doi.org/10.1038/ncomms15994>
- [31] H. Rostami, F. Guinea, M. Polini, and R. Roldán, npj 2D Materials and Applications. 2, (2018). <http://doi.org/10.1038/s41699-018-0061-7>
- [32] D. Kielpinski, C. Monroe and D.J. Wineland, Nature. 417, 709 (2002).
- [33] K. Wright, K.M. Beck, S. Debnath, J.M. Amini, Y. Nam, N. Grzesiak, J.S. Chen, N.C. Pisenti, M. Chmielewski, C. Collins, K.M. Hudek, J. Mizrahi, J.D. Wong-Campos, S. Allen, J. Apisdorf, P. Solomon, M. Williams, A.M. Ducore, A. Blinov, S.M. Kreikemeier, V. Chaplin, M. Keesan, C. Monroe, and J. Kim, Nat Commun. 10, 5464 (2019). <http://doi.org/10.1038/s41467-019-13534-2>
- [34] I. Pogorelov, T. Feldker, C.D. Marciak, L. Postler, G. Jacob, O. Kriegsteiner, V. Podlesnic, M. Meth, V. Negnevitsky, M. Stadler, B. Höfer, C. Wächter, K. Lakhmanskiy, R. Blatt, P. Schindler, and T. Monz, PRX Quantum. 2, (2021). <http://doi.org/10.1103/PRXQuantum.2.020343>

- [35] J.M. Pino, J.M. Dreiling, C. Figgatt, J.P. Gaebler, S.A. Moses, M.S. Allman, C.H. Baldwin, M. FossFeig, D. Hayes, K. Mayer, C. Ryan-Anderson, and B. Neyenhuis, *Nature*. 592, 209 (2021). <http://doi.org/10.1038/s41586-021-03318-4>
- [36] D. Hanneke, J.P. Home, J.D. Jost, J.M. Amini, D. Leibfried, and D.J. Wineland, *Nature Physics*. 6, 13 (2009). <http://doi.org/10.1038/nphys1453>
- [37] P. Schindler, D. Nigg, T. Monz, J.T. Barreiro, E. Martinez, S.X. Wang, S. Quint, M.F. Brandl, V. Nebendahl, C.F. Roos, M. Chwalla, M. Hennrich, and R. Blatt, *New Journal of Physics*. 15, (2013). <http://doi.org/10.1088/1367-2630/15/12/123012>
- [38] S.D. Fallek, C.D. Herold, B.J. McMahon, K.M. Maller, K.R. Brown, and J.M. Amini, *New Journal of Physics*. 18, (2016). <http://doi.org/10.1088/1367-2630/18/8/083030>
- [39] T. Monz, D. Nigg, E.A. Martinez, M.F. Brandl, P. Schindler, R. Rines, S.X. Wang, I.L. Chuang, and R. Blatt, *Science*. 351, 1068 (2016).
- [40] S. Debnath, N.M. Linke, C. Figgatt, K.A. Landsman, K. Wright, and C. Monroe, *Nature*. 536, 63 (2016). <http://doi.org/10.1038/nature18648>
- [41] N.M. Linke, D. Maslov, M. Roetteler, S. Debnath, C. Figgatt, K.A. Landsman, K. Wright, and C. Monroe, *Proceedings of the National Academy of Sciences*. 114, 3305 (2017). <http://doi.org/10.1073/pnas.1618020114>
- [42] C. Hempel, C. Maier, J. Romero, J. McClean, T. Monz, H. Shen, P. Jurcevic, B.P. Lanyon, P. Love, R. Babbush, A. Aspuru-Guzik, R. Blatt, and C.F. Roos, *Physical Review X*. 8, (2018). <http://doi.org/10.1103/PhysRevX.8.031022>
- [43] K.R. Brown, J. Chiaverini, J.M. Sage, and H. Häffner, *Nature Reviews Materials*. 6, 892 (2021). <http://doi.org/10.1038/s41578-021-00292-1>
- [44] T.D. Ladd, F. Jelezko, R. Laflamme, Y. Nakamura, C. Monroe, and J.L. O'Brien, *Nature*. 464, 45 (2010). <http://doi.org/10.1038/nature08812>
- [45] Q.A. Turchette, B. King, D. Leibfried, D. Meekhof, C. Myatt, M. Rowe, C. Sackett, C. Wood, W. Itano, and C. Monroe, *Physical Review A*. 61, 063418 (2000).
- [46] L. Deslauriers, S. Olmschenk, D. Stick, W.K. Hensinger, J. Sterk, and C. Monroe, *Physical Review Letters*. 97, (2006). <http://doi.org/10.1103/PhysRevLett.97.103007>
- [47] D. Berkeland, J. Miller, J.C. Bergquist, W.M. Itano, and D.J. Wineland, *Journal of applied physics*. 83, 5025 (1998).
- [48] M. Neek-Amal, L. Covaci and F.M. Peeters, *Physical Review B*. 86, (2012). <http://doi.org/10.1103/PhysRevB.86.041405>
- [49] J.A. Sedlacek, J. Stuart, D.H. Slichter, C.D. Bruzewicz, R. McConnell, J.M. Sage, and J. Chiaverini, *Physical Review A*. 98, (2018). <http://doi.org/10.1103/PhysRevA.98.063430>

- [50] D.A. Hite, Y. Colombe, A.C. Wilson, K.R. Brown, U. Warring, R. Jördens, J.D. Jost, K.S. McKay, D.P. Pappas, D. Leibfried, and D.J. Wineland, Physical Review Letters. 109, (2012). <http://doi.org/10.1103/PhysRevLett.109.103001>
- [51] C. Noel, M. Berlin-Udi, C. Matthiesen, J. Yu, Y. Zhou, V. Lordi, and H. Häffner, Physical Review A. 99, 063427 (2019). <http://doi.org/10.1103/PhysRevA.99.063427>
- [52] K.K. Mehta, C. Zhang, M. Malinowski, T.-L. Nguyen, M. Stadler, and J.P. Home, Nature. 586, 533 (2020). <http://doi.org/10.1038/s41586-020-2823-6>
- [53] D.J. Heinzen and D.J. Wineland, Phys Rev A. 42, 2977 (1990). <http://doi.org/10.1103/physreva.42.2977>
- [54] M. E, Quantum mechanics. (Jones & Bartlett Publishers,.1961)
- [55] M. Ilina, Y.F. Blinov, O. Ilin, N. Rudyk, and O. Ageev. *Piezoelectric effect in non-uniform strained carbon nanotubes.* in *IOP Conference Series: Materials Science and Engineering.* 2017. IOP Publishing.
- [56] Y. Niquet, C. Priester, C. Gourgon, and H. Mariette, Physical Review B. 57, 14850 (1998). <http://doi.org/10.1103/PhysRevB.57.14850>
- [57] X. Wang, W. Peng, R. Yu, H. Zou, Y. Dai, Y. Zi, C. Wu, S. Li, and Z.L. Wang, Nano Letters. 17, 3718 (2017). <http://doi.org/10.1021/acs.nanolett.7b01004>
- [58] X. Du, W. Tian, J. Pan, B. Hui, J. Sun, K. Zhang, and Y. Xia, Nano energy. 92, 106694 (2022). <http://doi.org/10.1016/j.nanoen.2021.106694>
- [59] S. Tu, Y. Guo, Y. Zhang, C. Hu, T. Zhang, T. Ma, and H. Huang, Advanced Functional Materials. 30, 2005158 (2020). <http://doi.org/10.1002/adfm.202005158>
- [60] R. Blakestad, C. Ospelkaus, A. VanDevender, J. Amini, J. Britton, D. Leibfried, and D.J. Wineland, Physical review letters. 102, 153002 (2009). <http://doi.org/10.1103/PhysRevLett.102.153002>
- [61] D. Leibrandt, J. Labaziewicz, R. Clark, I. Chuang, R. Epstein, C. Ospelkaus, J. Wesenberg, J. Bollinger, D. Leibfried, and D. Wineland, Quantum Information & Computation. 9, 901 (2009). <http://doi.org/10.5555/2012098.2012099>
- [62] P. Delsing, A.N. Cleland, M.J. Schuetz, J. Knörzer, G. Giedke, J.I. Cirac, K. Srinivasan, M. Wu, K.C. Balram, and C. Bäuerle, Journal of Physics D: Applied Physics. 52, 353001 (2019). <http://doi.org/10.1088/1361-6463/ab1b04>
- [63] V.J. Gokhale, B.P. Downey, D.S. Katzer, N. Nepal, A.C. Lang, R.M. Stroud, and D.J. Meyer, Nature communications. 11, 2314 (2020).
- [64] S.-H. Shin, Y.-H. Kim, J.-Y. Jung, M.H. Lee, and J. Nah, Nanotechnology. 25, 485401 (2014). <http://doi.org/10.1088/0957-4484/25/48/485401>
- [65] M.B. Khan, D.H. Kim, J.H. Han, H. Saif, H. Lee, Y. Lee, M. Kim, E. Jang, S.K. Hong, and D.J. Joe, Nano Energy. 58, 211 (2019). <http://doi.org/10.1016/j.nanoen.2019.01.049>

- [66] L. Gu, N. Cui, L. Cheng, Q. Xu, S. Bai, M. Yuan, W. Wu, J. Liu, Y. Zhao, and F. Ma, Nano letters. 13, 91 (2013). <http://doi.org/10.1021/nl303539c>
- [67] A.K. Zak and W.A. Majid, Ceramics International. 37, 753 (2011). <http://doi.org/10.1016/j.ceramint.2010.10.020>
- [68] G.H. Khorrami, A.K. Zak and A. Kompany, Ceramics International. 38, 5683 (2012). <http://doi.org/10.1016/j.ceramint.2012.04.012>
- [69] A. Scalabrin, A. Chaves, D. Shim, and S. Porto, physica status solidi (b). 79, 731 (1977). <http://doi.org/10.1002/pssb.2220790240>
- [70] R.A. Evarestov and A.V. Bandura, Journal of computational chemistry. 33, 1123 (2012). <http://doi.org/10.1002/jcc.22942>
- [71] S.M. Park, B. Wang, T. Paudel, S.Y. Park, S. Das, J.R. Kim, E.K. Ko, H.G. Lee, N. Park, L. Tao, D. Suh, E.Y. Tsymbal, L.Q. Chen, T.W. Noh, and D. Lee, Nat Commun. 11, 2586 (2020). <http://doi.org/10.1038/s41467-020-16207-7>
- [72] A. Jayaraman, Reviews of Modern Physics. 55, 65 (1983). <http://doi.org/10.1103/RevModPhys.55.65>
- [73] Y. Wang, X. Lü, W. Yang, T. Wen, L. Yang, X. Ren, L. Wang, Z. Lin, and Y. Zhao, Journal of the American Chemical Society. 137, 11144 (2015). <http://doi.org/10.1021/jacs.5b06346>
- [74] Z. Jenei, E. O'Bannon, S. Weir, H. Cynn, M. Lipp, and W. Evans, Nature communications. 9, 3563 (2018). <http://doi.org/10.1038/s41467-018-06071-x> |
- [75] M.-W. Chu, I. Szafraniak, R. Scholz, C. Harnagea, D. Hesse, M. Alexe, and U. Gösele, Nature materials. 3, 87 (2004). <http://doi.org/10.1038/NMAT1057>
- [76] E. Oksenberg, A. Merdasa, L. Houben, I. Kaplan-Ashiri, A. Rothman, I.G. Scheblykin, E.L. Unger, and E. Joselevich, Nature communications. 11, 489 (2020). <http://doi.org/10.1038/s41467-020-14365-2>
- [77] C. Zhu, X. Niu, Y. Fu, N. Li, C. Hu, Y. Chen, X. He, G. Na, P. Liu, and H. Zai, Nature communications. 10, 815 (2019). <http://doi.org/10.1038/s41467-019-08507-4>
- [78] Y. Zhang, G. Hu, Y. Zhang, L. Li, M. Willatzen, and Z.L. Wang, Nano Energy. 60, 649 (2019). <http://doi.org/10.1016/j.nanoen.2019.04.011>
- [79] T. Liu, D. Li, H. Hu, X. Huang, Z. Zhao, W. Sha, C. Jiang, C. Du, M. Liu, and X. Pu, Nano Energy. 67, 104218 (2020). <http://doi.org/10.1016/j.nanoen.2019.104218>
- [80] Z.L. Wang, Materials Today. 52, 348 (2022). <http://doi.org/10.1016/j.mattod.2021.10.027>

## Figure caption

**Fig. 1** (a) The structure of the ion trap, showing direct current electrodes, radio-frequency (RF) electrodes, and electrically floating wire (gold areas). (b) The low part shows the potential distribution along trap  $x$  axis. The ion positions are marked by red spheres, with trapping wells separated by 40  $\mu\text{m}$ . The electrodes are enough to control position axis of ions and frequency. Both the original motional frequency are  $\sim 4$  MHz.

**Fig. 2** Energy level and wave function for harmonic oscillators. (a) Bound-state solutions, without strain (left), positive strain gradient (centre), and negative strain gradient (right). The orange region is the states of quantum oscillators. In this figure, we consider to show situation with four bound state in total. Without strain, we show the energy level of the quantized modes because of axis oscillatory motion. They are separated by  $\hbar\omega_0$  in energy space. In this figure, it is shown for the energy level corresponded to  $E_0, E_1, E_2, E_3$ . Under nonuniform strain, the motional frequency of quantum oscillators can be increased or decreased due to nonlinear potential induced by positive or negative strain gradient. For clarity, we show the change of ground state energy ( $\hbar\omega_{\text{piezo}}$ ) owing to strain gradient. (b) Bound-state solutions for a motional frequency  $\omega_0=4.04$  MHz. The diagonal straight lines show approximately linear region. (c) Normalized squared wavefunctions  $|\psi_0|^2$  for bound state solution of strain gradient choice  $s_{33,3}=0$  and  $s_{33,3}=0.2$ . The corresponding energy is  $E_0=\hbar\omega/2$ . The dotted lines show the region of higher  $|\psi_0|^2$  under strain gradient. (d) Normalized squared wavefunctions  $|\psi_0|^2$  of two trapped ions separated by a distance  $s_0=40$   $\mu\text{m}$ . A ground state in the left trapped ion is coupled to a ground state in the right trapped ion. The coupling is  $\Omega_{\text{ex}} \propto 1/\omega_0$ , where is the motional frequency under resonance condition. Furthermore, the trapped ions highly localized, it is seen from the ratio  $P(\text{in})/P(\text{out})$ .  $P(\text{in})$  is the probability of the ion inside the trapping wells and  $P(\text{out})$  is probability outside the trapping wells. The parameters chosen for the quantized mechanical oscillators are  $s_{33,3}=0.2$ ,  $\omega_0/2\pi \approx 4.04$  MHz.

**Fig. 3** Performance of trapped ions under strain gradient. (a) Structure and strain distribution under nonuniform strain; (b) Time of energy swapping. (c) The coupling rate. (d) Relative surface electric field noise at the bound-state solution of parameter choice  $\alpha$  arrange from -1.5 to -1.0.

**Fig. 4** Motional frequency and relative surface electric field noise under different ion's separated distance. a,b The motional frequency (a), Relative surface electric field noise ( $S_{E,\text{piezo}}/S_E$ ) (b). The boundstate solution of parameter choice  $\omega_0=4.04$  MHz. Frequency and period of energy swapping under different ion's separated distance. c,d  $\Omega_{\text{ex}}/\pi$  (c),  $\tau_{\text{ex}}$ (d).

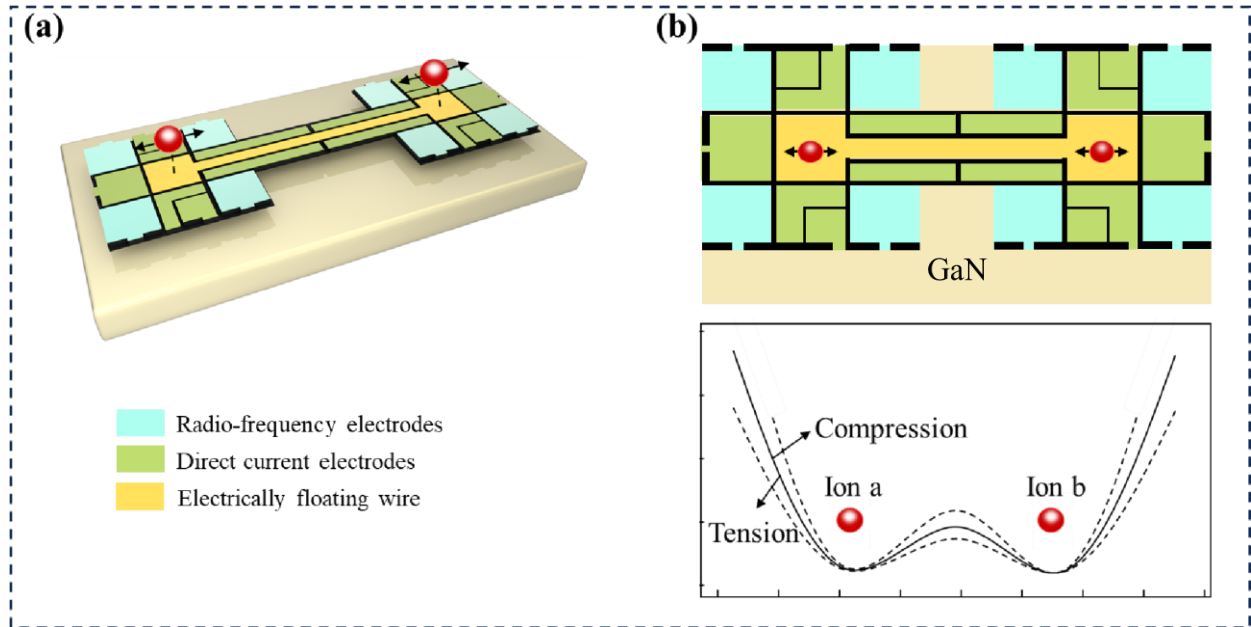
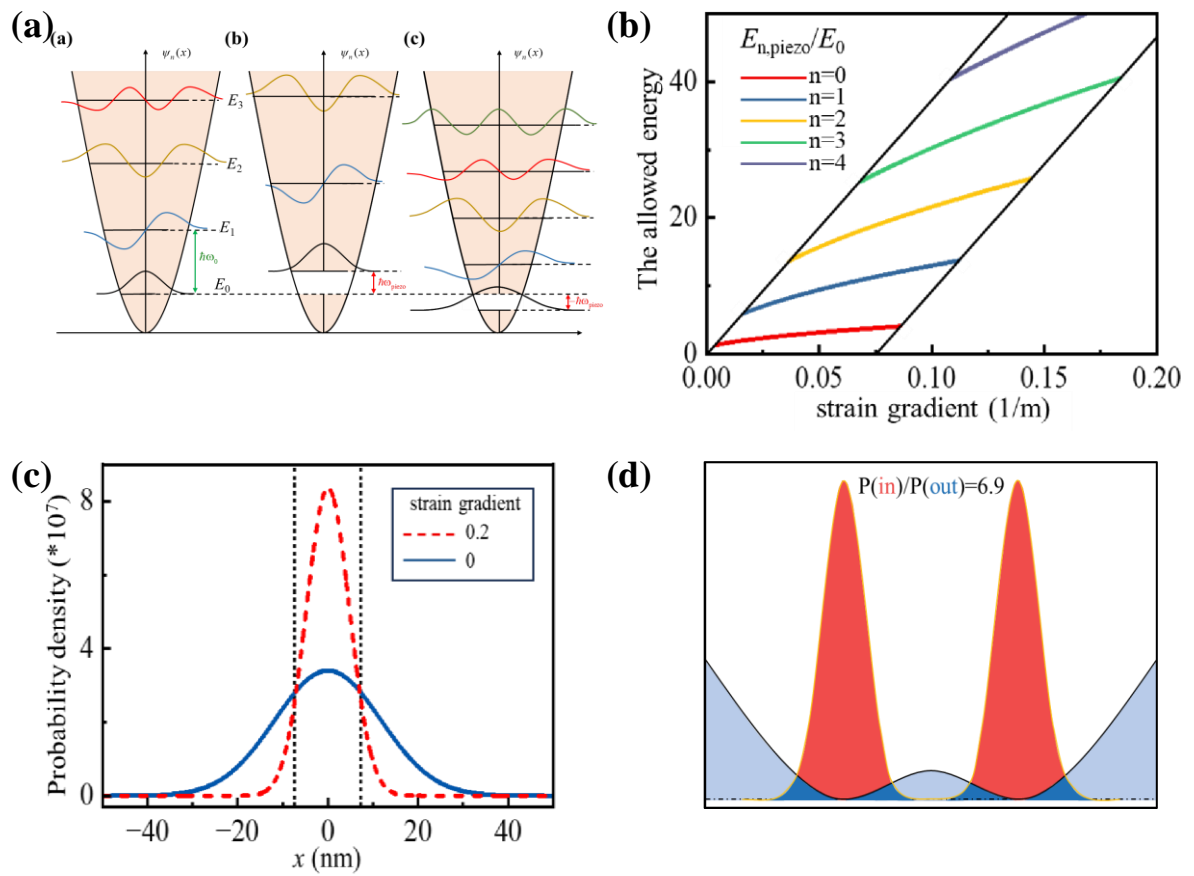
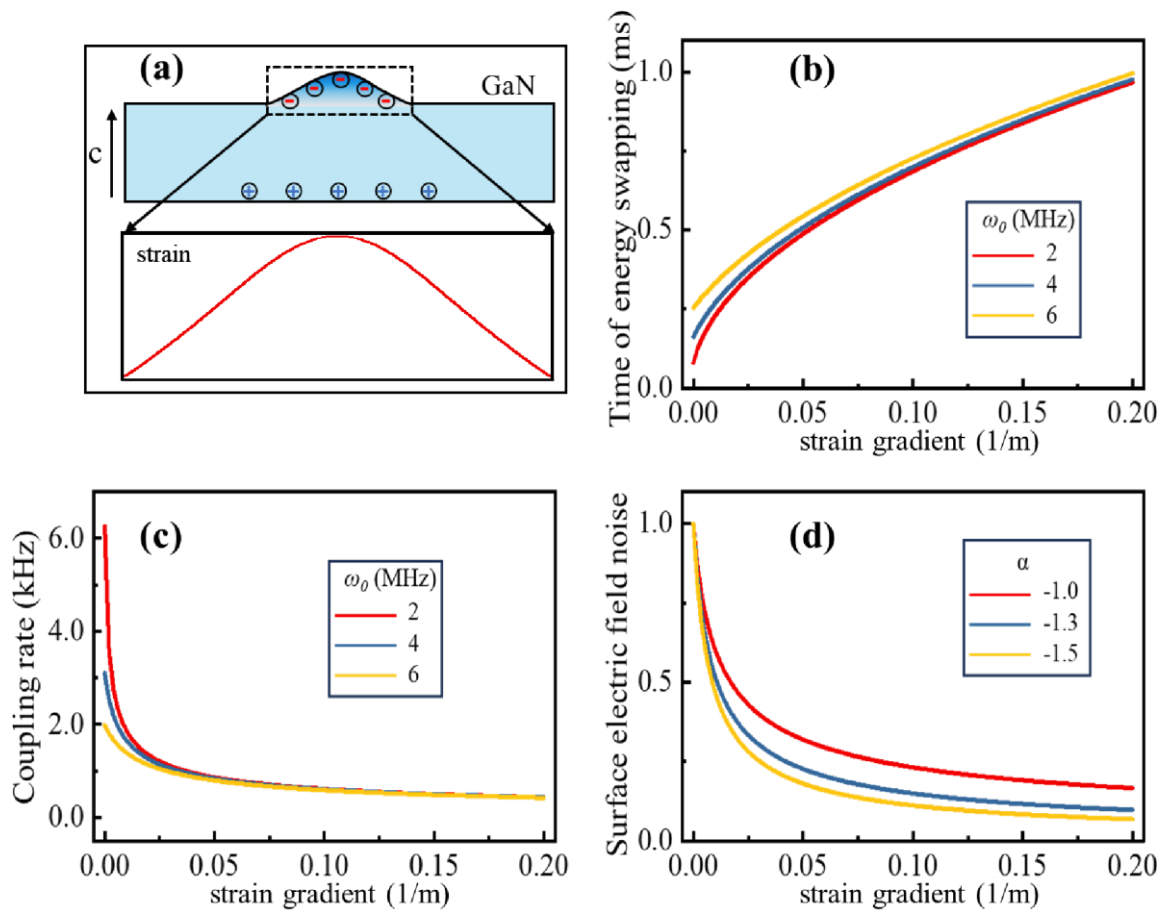


Fig. 1



**Fig. 2**



**Fig. 3**

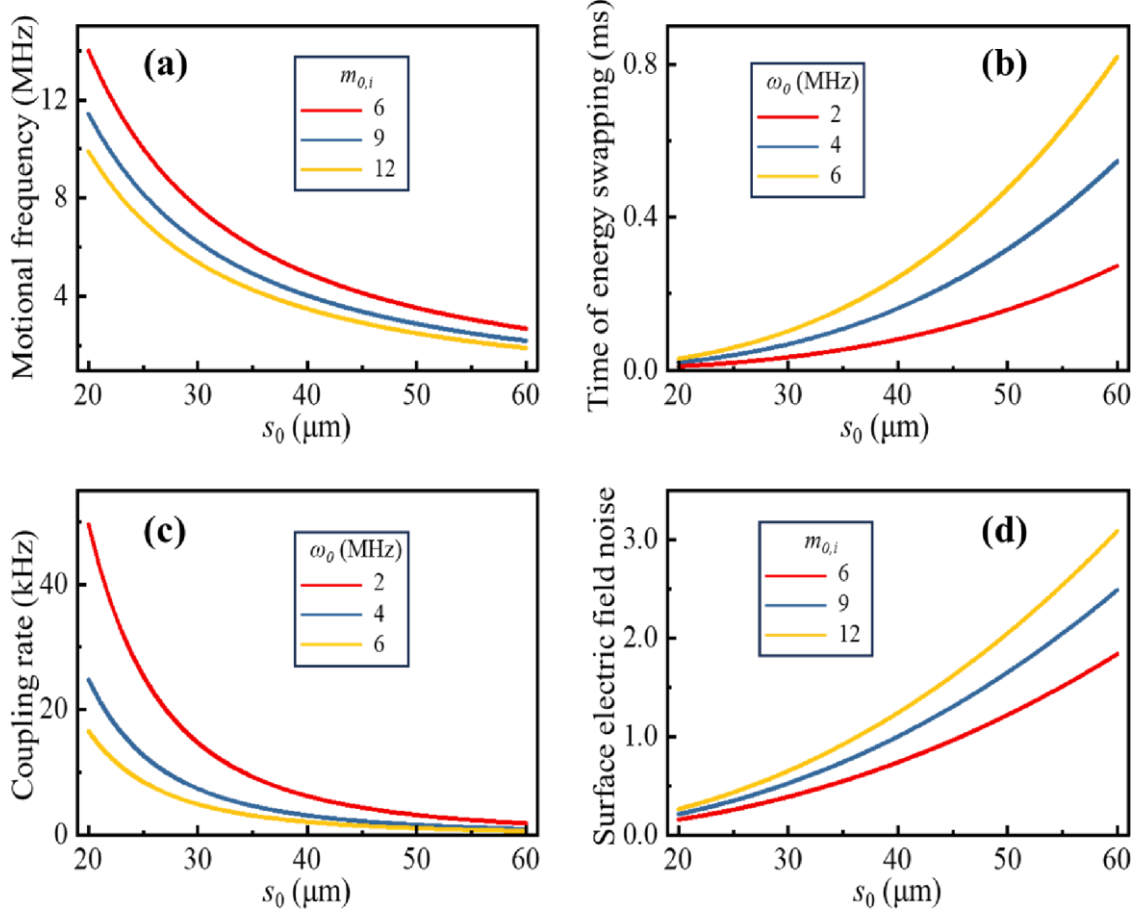


**Fig. 4**